

Preliminary analysis of $K \rightarrow \pi\pi$ with 2+1 flavor DWF lattices on QCDOC

RBC and UKQCD Collaborations: Shu Li*

Department of Physics, Columbia University, New York, NY 10027, USA

E-mail: lishu@phys.columbia.edu

We present a progress report on the calculation of the $K \rightarrow \pi\pi$ weak matrix elements on the RBC/UKQCD 2+1 flavor dynamical DWF lattices. For this calculation, the relevant $K \rightarrow \pi$ matrix elements are calculated and renormalized in the RI/MOM scheme. We have tried using leading-order chiral perturbation theory to extrapolate the matrix elements and this effort eventually shows the necessity of obtaining the next-to-leading order partially quenched chiral perturbation theory for non-degenerate sea quark masses. The analysis is conducted on $16^3 \times 32$ lattices.

XXIVth International Symposium on Lattice Field Theory

July 23-28, 2006

Tucson, Arizona, USA

*Speaker.

1. Introduction and Motivation

The creation of a new generation of computer hardware and software has given us deeper insight into challenging problems, such as CP violation. Based on the recent analysis of the CP violating weak decay process $K \rightarrow \pi\pi$ on quenched lattices[1, 2], we are conducting a comparable research program on the latest 2+1 flavor dynamical lattices.

Calculating $\text{Re}(\varepsilon'/\varepsilon)$ requires evaluating the weak matrix elements $A_2 = \langle \pi\pi | \mathcal{O}^{\Delta I=3/2} | K \rangle$ and $A_0 = \langle \pi\pi | \mathcal{O}^{\Delta I=1/2} | K \rangle$, where $\mathcal{O}^{\Delta I=3/2}$ and $\mathcal{O}^{\Delta I=1/2}$ are the low-energy four-quark operators with quantum number $\Delta S = 1$. On the lattice, it is often easier to use chiral perturbation theory (χPT) to relate the $K \rightarrow \pi\pi$ matrix elements to simpler $K \rightarrow \pi$ and $K \rightarrow \text{vacuum}$ matrix elements.

2. Operators

In 3-flavor QCD, we can expand the weak Hamiltonian responsible for $K \rightarrow \pi\pi$ decay into 10 low-energy four-quark operators. And we can further divide them into a $\Delta I = 3/2$ part and a $\Delta I = 1/2$ part. There are 6 operators that have a $\Delta I = 3/2$ part: $\{ \mathcal{O}_i^{(3/2)} | i = 1, 2, 7, 8, 9, 10 \}$. In this set, 4 operators are all proportional to a single operator $\mathcal{O}^{(27,1)(3/2)}$, that $\mathcal{O}^{(27,1)(3/2)} = 3\mathcal{O}_{1,2}^{(3/2)} = 2\mathcal{O}_{9,10}^{(3/2)}$. By definition,

$$\mathcal{O}^{(27,1)(3/2)} \equiv (\bar{s}_\alpha d_\alpha)_L (\bar{u}_\beta u_\beta)_L + (\bar{s}_\alpha u_\alpha)_L (\bar{u}_\beta d_\beta)_L - (\bar{s}_\alpha d_\alpha)_L (\bar{d}_\beta d_\beta)_L \quad (2.1)$$

where α and β are color indices. The two remaining operators are

$$\mathcal{O}_7^{(3/2)} \equiv (\bar{s}_\alpha d_\alpha)_L (\bar{u}_\beta u_\beta)_R + (\bar{s}_\alpha u_\alpha)_L (\bar{u}_\beta d_\beta)_R - (\bar{s}_\alpha d_\alpha)_L (\bar{d}_\beta d_\beta)_R \quad (2.2)$$

$$\mathcal{O}_8^{(3/2)} \equiv (\bar{s}_\alpha d_\beta)_L (\bar{u}_\beta u_\alpha)_R + (\bar{s}_\alpha u_\beta)_L (\bar{u}_\beta d_\alpha)_R - (\bar{s}_\alpha d_\beta)_L (\bar{d}_\beta d_\alpha)_R \quad (2.3)$$

For these $\Delta I = 3/2$ operators, from χPT , evaluating their $K \rightarrow \pi$ matrix elements is sufficient to determine their $K \rightarrow \pi\pi$ matrix elements to leading order in mass and momentum.

3. Simulation Details

We have measured our matrix elements on the RBC/UKQCD 2+1 flavor dynamical lattices, using the Iwasaki gauge action with $\beta = 2.13$ and domain wall fermions with $L_s = 16$. The lattice spacing is $a^{-1} = 1.60(3) \text{ GeV}$ and the residual mass $m_{\text{res}} \sim 0.003$ in lattice units.

We have set $m_{s,\text{sea}} = 0.04$ and we have three choices for the light sea quark masses, which are $m_{u,\text{sea}} = m_{d,\text{sea}} \in \{0.01, 0.02, 0.03\}$. Thus we have generated three independent ensembles. On each ensemble we have collected 75 configurations, each separated by 40 trajectories. And we have 5 choices for valance quark masses, which are $m_{q,\text{val}} \in \{0.01, 0.02, 0.03, 0.04, 0.05\}$.

4. Evaluation of $K \rightarrow \pi$ Matrix Elements

4.1 Matrix Elements from Green's Functions

To evaluate the $K \rightarrow \pi$ matrix elements, we put wall sources at $t_K = 5$ and $t_\pi = 27$, and take the ratio of the wall-wall three-point Green's function $G_{\pi\mathcal{O}K}(t; t_K, t_\pi)$ with wall-point two-point

Green's functions $G_\pi(t; t_\pi)$ and $G_K(t; t_K)$ [1]:

$$\lim_{t_\pi \gg t \gg t_K} \frac{G_{\pi\mathcal{O}K}(t; t_K, t_\pi)}{G_\pi(t; t_\pi) G_K(t; t_K)} \rightarrow \frac{\langle \pi^+ | \mathcal{O} | K^+ \rangle}{\langle \pi^+ | \mathcal{P}_{\pi^-} | 0 \rangle \langle 0 | \mathcal{P}_{K^+} | K^+ \rangle} \quad (4.1)$$

where $\mathcal{P}_{\pi^-}(x) \equiv [i\bar{u}\gamma_5 d](x)$ and $\mathcal{P}_{K^+}(x) \equiv [i\bar{s}\gamma_5 u](x)$.

Then, to remove the denominator, we make use of the wall-point two-point functions together with the wall-wall two-point functions:

$$\lim_{t_\pi \gg t} G_\pi^{WP} = \frac{1}{2m_\pi} \langle 0 | \chi_{\pi^+} | \pi^+ \rangle \langle \pi^+ | \mathcal{P}_{\pi^-} | 0 \rangle e^{-m_\pi(t_\pi - t)} \quad (4.2)$$

$$\lim_{t_\pi \gg t} G_\pi^{WW} = \frac{1}{2m_\pi} |\langle 0 | \chi_{\pi^+} | \pi^+ \rangle|^2 e^{-m_\pi(t_\pi - t)} \quad (4.3)$$

where $\langle 0 | \chi_{\pi^+} | \pi^+ \rangle$ is the normalization factor of the wall source, and $\langle \pi^+ | \mathcal{P}_{\pi^-} | 0 \rangle$ is that of the point source. With simultaneous fitting, we can calculate the required matrix elements from Eq (4.1), (4.2) and (4.3).

5. Non-Perturbative Renormalization

To renormalize the $K \rightarrow \pi$ matrix elements, we follow the Rome-Southampton RI/MOM prescription described in [1], with $ap_i = \frac{2\pi n_i}{L_i}$. On our lattices, $L_x = L_y = L_z = 16$ and $L_t = 32$. And the value of momenta is: $n_x, n_y \in \{-2, -1, 0, 1, 2\}$, $n_z \in \{0, 1, 2\}$ and $n_t \in \{0, 1, 2, 3, 4\}$.

If \mathcal{O}^i is a four-quark operator, and E^j is a combination of external quark fields with definite spin and color structure, and Fourier transformed into momentum space,

$$E_{\alpha\beta\gamma\delta}^j = f^{j,abcd} q_\alpha^a(p_1) \bar{q}_\beta^b(p_2) q_\gamma^c(p_1) \bar{q}_\delta^d(p_2) \quad (5.1)$$

the renormalization condition between \mathcal{O}^i and E^j is:

$$Z_q^{-2} Z^{ki} P^j \{ \Lambda^{i,j} \} = F^{kj} \quad (5.2)$$

where $\Lambda^{i,j}$ is the amputated Green's function with operator \mathcal{O}^i connected with the external quark fields in E^j . And P^j is a suitable projector, which corresponds to the spin structure of E^j . The quantity F^{kj} is the tree-level counterpart of $P^j \{ \Lambda^{i,j} \}$ evaluated in the free-field limit. Note there is no sum on j in the above equation. The momentum are chosen such that $p_1^2 = p_2^2 = |p_1 - p_2|^2 = \mu^2$. After getting the value of $Z_q^{-2} Z^{ki}$ at certain momentum scale μ and quark mass m_q , we then multiply it by Z_q^2 , obtained by NPR of axial current, with the method detailed in [3], to get the final renormalization matrix Z^{ki} .

5.1 Non-Perturbative Renormalization for $\mathcal{O}^{(27,1)(3/2)}$

On DWF lattices, chirality is approximately conserved ($m_{\text{res}} \ll \Lambda_{\text{QCD}}$), so $\mathcal{O}^{(27,1)(3/2)}$ doesn't mix with the operators of different chirality, and we can neglect the mixing coefficients, keeping only the diagonal element,

$$\mathcal{O}_{\text{ren}}^{(27,1)(3/2)} = Z^{(27,1)(3/2)} \mathcal{O}_{\text{lat}}^{(27,1)(3/2)} \quad (5.3)$$

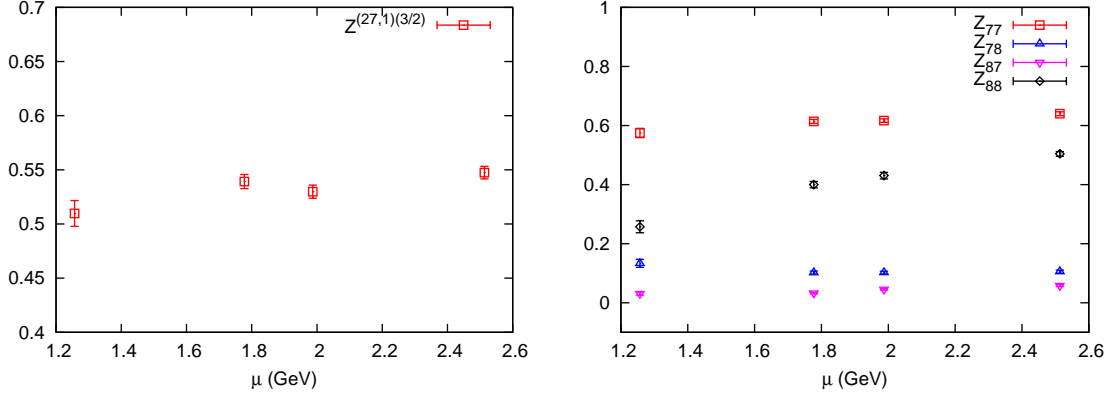


Figure 1: Renormalization factors $Z^{(27,1)(3/2)}$ (left) and individual elements of $Z^{(8,8)(3/2)}$ (right) at several momentum scale μ .

Table 1: Renormalization factors $Z^{(27,1)(3/2)}$ and individual elements of $Z^{(8,8)(3/2)}$ at several momentum scale μ .

p_{latt}^2	μ (GeV)	$Z^{(27,1)(3/2)}$	Z_{77}	Z_{78}	Z_{87}	Z_{88}
0.617	1.257	0.510(12)	0.575(16)	0.133(14)	0.0310(52)	0.257(20)
1.234	1.777	0.5392(65)	0.6139(67)	0.1021(52)	0.0326(30)	0.400(11)
1.542	1.987	0.5298(60)	0.6167(58)	0.1021(47)	0.0453(27)	0.430(11)
2.467	2.513	0.5474(58)	0.6400(66)	0.1053(54)	0.0579(34)	0.5040(80)

After quadratic fitting in quark masses, the quantity $Z^{(27,1)(3/2)}$ in the massless limit and for several values of μ is plotted in Fig 1 and listed in Table 1. One should note that the renormalization constant $Z^{(27,1)(3/2)}$ is related to the renormalization constant for B_K . By definition, $Z_{B_K} = Z_{LL}/Z_A^2$, where Z_{LL} is the same as $Z^{(27,1)(3/2)}$ if we change the choice of momentum in Eq (5.1) into $p_1 = p_2$, which we have verified.

5.2 Non-Perturbative Renormalization for $\mathcal{O}_7^{(3/2)}$ and $\mathcal{O}_8^{(3/2)}$

Different from the case of $\mathcal{O}^{(27,1)(3/2)}$, these two operators mix with each other on lattice. So their renormalization coefficients form a 2×2 matrix $Z^{(8,8)(3/2)}$,

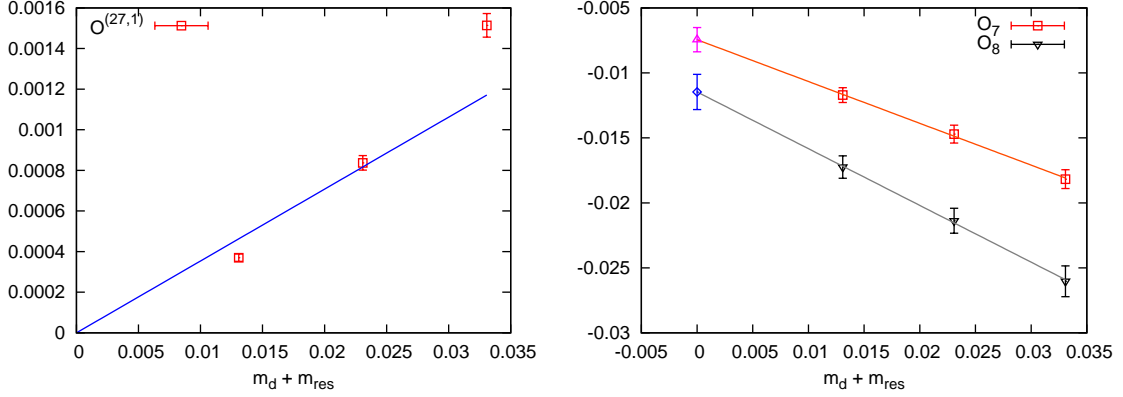
$$\begin{pmatrix} \mathcal{O}_{7,\text{ren}}^{(3/2)} \\ \mathcal{O}_{8,\text{ren}}^{(3/2)} \end{pmatrix} = \begin{pmatrix} Z_{77} & Z_{78} \\ Z_{87} & Z_{88} \end{pmatrix} \begin{pmatrix} \mathcal{O}_{7,\text{lat}}^{(3/2)} \\ \mathcal{O}_{8,\text{lat}}^{(3/2)} \end{pmatrix} \quad (5.4)$$

Following the same prescription as in Section 5.1, we can calculate the mixing matrix $Z^{(8,8)(3/2)}$ at various external momentum scale. The individual elements of $Z^{(8,8)(3/2)}$ are also plotted in Fig 1 and listed in Table 1.

Now we can renormalize the matrix elements $\langle \pi^+ | \mathcal{O}^{(27,1)(3/2)} | K^+ \rangle$, $\langle \pi^+ | \mathcal{O}_7^{(3/2)} | K^+ \rangle$ and $\langle \pi^+ | \mathcal{O}_8^{(3/2)} | K^+ \rangle$. Their values at one scale $\mu = 1.99\text{GeV}$ are listed in Table 2.

Table 2: RI/MOM renormalized matrix elements $\langle \pi^+ | \mathcal{O}^{(27,1)(3/2)} | K^+ \rangle$, $\langle \pi^+ | \mathcal{O}_7^{(3/2)} | K^+ \rangle$ and $\langle \pi^+ | \mathcal{O}_8^{(3/2)} | K^+ \rangle$, at $\mu = 1.99\text{GeV}$, in lattice units.

m_{sea}	m_{val}	$\mathcal{O}^{(27,1)(3/2)}$	$\mathcal{O}_7^{(3/2)}$	$\mathcal{O}_8^{(3/2)}$
0.01/0.04	0.01/0.01	$3.70(18) \times 10^{-4}$	$-1.171(57) \times 10^{-2}$	$-1.724(86) \times 10^{-2}$
0.02/0.04	0.02/0.02	$8.37(36) \times 10^{-4}$	$-1.471(69) \times 10^{-2}$	$-2.138(96) \times 10^{-2}$
0.03/0.04	0.03/0.03	$1.514(58) \times 10^{-3}$	$-1.817(72) \times 10^{-2}$	$-2.60(12) \times 10^{-2}$

**Figure 2:** A fit of the renormalized matrix elements $\langle \pi^+ | \mathcal{O}^{(27,1)(3/2)} | K^+ \rangle$ (left) and $\langle \pi^+ | \mathcal{O}_{7,8}^{(3/2)} | K^+ \rangle$ (right) to leading-order χPT . The data points are from quarks with masses $m_{d,\text{val}} = m_{s,\text{val}} = m_{d,\text{sea}}$. (a) The fit for $\mathcal{O}^{(27,1)(3/2)}$ shows the leading-order theory is not sufficient ($\chi^2/d.o.f \sim 30$). (b) The phenomenological fit for \mathcal{O}_7 and \mathcal{O}_8 takes an inexact “chiral limit” since $m_{s,\text{sea}} = 0.04 + m_{\text{res}}$ remains non-zero, and thus the value at that limit has an unknown systematic error.

6. Chiral Extrapolation

6.1 Chiral Fit for $\mathcal{O}^{(27,1)(3/2)}$

When we use degenerate valance quarks $m_{d,\text{val}} = m_{s,\text{val}}$, the leading order term in the χPT formula for $\langle \pi^+ | \mathcal{O}^{(27,1)(3/2)} | K^+ \rangle$ reduces to a linear form which goes through the origin [1, 4],

$$\left\langle \pi^+ \left| \mathcal{O}^{(27,1)(3/2)} \right| K^+ \right\rangle_{\text{LO}} = -\frac{4}{f^2} \alpha^{(27,1)} B_0 m_{\text{val}} \quad (6.1)$$

Here we just show that this leading order approximation is not sufficient (Fig 2). We have used the data points where $m_{d,\text{val}} = m_{s,\text{val}} = m_{d,\text{sea}}$, and they have a large deviation from a straight line ($\chi^2/d.o.f \sim 30$), showing some quadratic behavior (note that the NLO term is expected to be a quadratic term of m_{val}^2 plus a chiral log term). The work to include the NLO terms is underway.

6.2 Chiral Fit for $\mathcal{O}_7^{(3/2)}$ and $\mathcal{O}_8^{(3/2)}$

Since these two operators are in (8,8) representation of the $SU(3)_L \otimes SU(3)_R$ group, the leading-order term for these operators is a constant,

$$\left\langle \pi^+ \left| \mathcal{O}^{(8,8)(3/2)} \right| K^+ \right\rangle_{\text{LO}} = \frac{4}{f^2} \alpha^{(8,8)} \quad (6.2)$$

Table 3: Leading-order LECs for $\mathcal{O}^{(8,8)(3/2)}$ operators in physical units: GeV^6 .

$\alpha_i^{(8,8)}$	$\mu = 1.26\text{GeV}$	$\mu = 1.78\text{GeV}$	$\mu = 1.99\text{GeV}$	$\mu = 2.51\text{GeV}$
7	$-1.97(26) \times 10^{-4}$	$-1.84(23) \times 10^{-4}$	$-1.85(23) \times 10^{-4}$	$-1.91(24) \times 10^{-4}$
8	$-1.71(22) \times 10^{-4}$	$-2.62(31) \times 10^{-4}$	$-2.84(34) \times 10^{-4}$	$-3.33(40) \times 10^{-4}$

Table 4: Matrix elements $\langle \pi^+\pi^- | \mathcal{O}_i^{(8,8)(3/2)} | K^0 \rangle$ in physical units: GeV^3 .

$\langle \pi^+\pi^- \mathcal{O}_i^{(8,8)(3/2)} K^0 \rangle$	$\mu = 1.26\text{GeV}$	$\mu = 1.78\text{GeV}$	$\mu = 1.99\text{GeV}$	$\mu = 2.51\text{GeV}$
7	0.289(38)	0.269(34)	0.270(34)	0.279(35)
8	0.251(33)	0.384(46)	0.416(49)	0.488(58)

At present, there is no publication on NLO partially quenched chiral perturbation theory (PQ χ PT) for $\mathcal{O}^{(8,8)}$ with non-degenerate sea quark masses. Thus, we retreat to phenomenological approach and from the distribution of the data points (Fig 2), and experiences on quenched lattices[1], we try to fit a straight line through the data points to extrapolate to chiral limit.

We should note that the ‘‘chiral limit’’ we extrapolate to is not the exact chiral limit of PQ χ PT (where all $m_q = 0$). The reason is our 2+1 flavor ensemble has a fixed $m_{s,\text{sea}} = 0.04 + m_{\text{res}}$ and cannot be extrapolated to zero. Therefore the extrapolated result at our ‘‘chiral limit’’ would have an unknown systematic error, which, again, could only be removed by NLO PQ χ PT.

Finally we find the LEC $\alpha_i^{(8,8)}$, $\{i = 7, 8\}$, as listed in Table 3. We use the leading-order χ PT formula, Eq (6.3) [4], to calculate $K \rightarrow \pi\pi$ matrix elements for $\mathcal{O}_i^{(8,8)}$, as in Table 4.

$$\langle \pi^+\pi^- | \mathcal{O}^{(8,8)(3/2)} | K^0 \rangle_{\text{LO}} = -\frac{4i}{f_K f_\pi^2} \alpha^{(8,8)} \quad (6.3)$$

7. Comparison with Quenched Results

In Fig 3, we have a preliminary comparison with the earlier RBC results[1] for the matrix elements $\langle \pi^+\pi^- | \mathcal{O}_i^{(3/2)} | K^0 \rangle$, $i \in \{7, 8\}$. Please note that the 2+1 flavor values are very preliminary results and still need to be thoroughly checked by independent calculations. So this comparison is not conclusive.

8. Conclusion and Outlook

Using RBC/UKQCD 2+1 flavor dynamical lattices of size $16^3 \times 32$ we have evaluated $K \rightarrow \pi$ matrix elements with the operators $\mathcal{O}^{(27,1)(3/2)}$, $\mathcal{O}_7^{(3/2)}$ and $\mathcal{O}_8^{(3/2)}$, and have calculated the relevant renormalization constants in the RI/MOM scheme. All of these matrix elements need further theoretical input from PQ χ PT.

The work on this project is continuing. We will also calculate the $\Delta I = 1/2$ matrix elements and gather more physical results, such as $\Delta I = 1/2$ rule and $\text{Re}(\epsilon'/\epsilon)$.

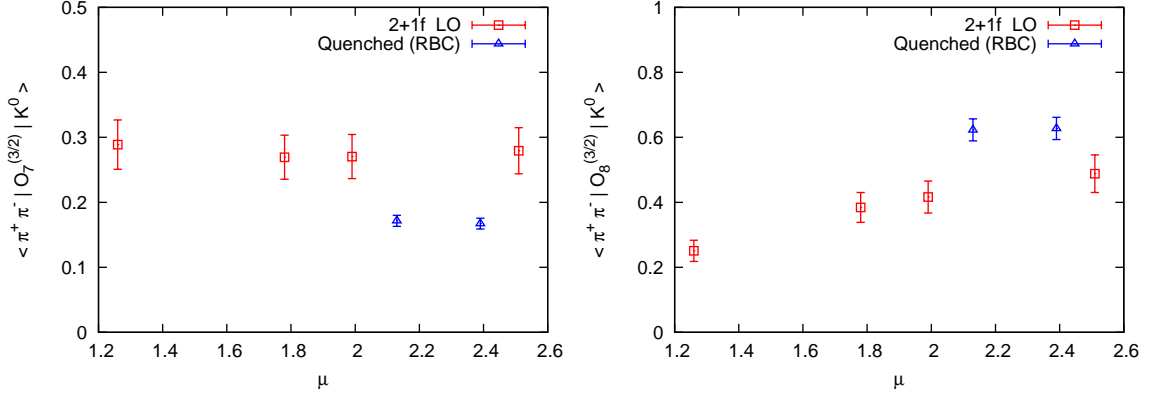


Figure 3: Comparison of matrix elements $\langle \pi^+ \pi^- | O_7^{(3/2)} | K^0 \rangle$ (left) and $\langle \pi^+ \pi^- | O_8^{(3/2)} | K^0 \rangle$ (right) with earlier RBC quenched results. The values are in physical units GeV^3 . The squares are the preliminary leading order value on 2+1 flavor lattice, and the triangles are the numbers in the RBC paper[1]. Note there is an unknown systematic error involved in 2+1 flavor value, due to the absence of NLO $PQ\chi PT$, that cannot be plotted.

Acknowledgment

Thanks to Norman Christ, Chris Dawson, Jack Laiho and Amarjit Soni for enlightening and helpful discussions. Thanks to Saul Cohen for help generating the datasets used in this work. Thanks to Peter Boyle, Dong Chen, Norman Christ, Mike Clark, Saul Cohen, Calin Cristian, Zhi-hua Dong, Alan Gara, Andrew Jackson, Balint Joo, Chulwoo Jung, Richard Kenway, Changhoan Kim, Ludmila Levkova, Huey-Wen Lin, Xiaodong Liao, Guofeng Liu, Robert Mawhinney, Shigemi Ohta, Tilo Wettig and Azusa Yamaguchi for the development of QCDOC hardware and its software.

The development and the resulting computer equipment were funded by the U.S. DOE grant DE-FG02-92ER40699, PPARC JIF grant PPA/J/S/1998/00756 and by RIKEN. This work was supported by U.S. DOE grant DE-FG02-92ER40699 and we thank RIKEN, BNL and the U.S. DOE for providing the facilities essential for this work.

References

- [1] T. Blum *et al.* (RBC), Phys. Rev. **D68**, 114506 (2003), hep-lat/0110075.
- [2] J. I. Noaki *et al.* (CP-PACS), Phys. Rev. **D68**, 014501 (2003), hep-lat/0108013.
- [3] T. Blum *et al.*, Phys. Rev. **D66**, 014504 (2002), hep-lat/0102005.
- [4] J. Laiho and A. Soni, Phys. Rev. **D71**, 014021 (2005), hep-lat/0306035.